

Electrically driven nematic flow in microfluidic devices containing a temperature gradient

A. V. Zakharov*

Saint Petersburg Institute for Machine Sciences, The Russian Academy of Sciences, Saint Petersburg 199178, Russia

P. V. Maslennikov[†]

Immanuel Kant Baltic Federal University, Kaliningrad 236040, Strasse Universitetskaya 2, Russia

S. V. Pasechnik[‡]

Moscow Technological University (MIREA), Moscow 119454, Russia



(Received 10 February 2020; accepted 21 May 2020; published 8 June 2020)

Fluid pumping principle has been developed utilizing the interaction, on the one hand, between the electric field \mathbf{E} and the gradient $\nabla \hat{\mathbf{n}}$ of the director's field, and, on the other hand, between the $\nabla \hat{\mathbf{n}}$ and the temperature ∇T gradient arising in a homogeneously aligned liquid crystal (HALC) microfluidic channel. Calculations, based upon the nonlinear extension of the classical Ericksen-Leslie theory, with accounting the entropy balance equation, show that due to the coupling among the ∇T , $\nabla \hat{\mathbf{n}}$, and \mathbf{E} in the HALC microfluidic channel the horizontal flow $\mathbf{v} = v_x \hat{\mathbf{i}} = u \hat{\mathbf{i}}$ may be excited. The direction and magnitude of \mathbf{v} is influenced both by the heat flux \mathbf{q} across the microfluidic channel and the strength of the electric field \mathbf{E} . The results of calculations showed that the dependence of the maximum value of the equilibrium velocity distribution $|u_{\max}(E/E_{\text{th}})|$ across the LC channel versus electric field E/E_{th} is characterized by maximum value at $E/E_{\text{th}} = 2.0$. In the case when the electric field $E \gg E_{\text{th}}$, the horizontal flow of the LC material completely stops and a novel mechanism of converting of the electric field in the form of the kinklike wave reorientation of the director field $\hat{\mathbf{n}}$ can be excited in the LC channel.

DOI: [10.1103/PhysRevE.101.062702](https://doi.org/10.1103/PhysRevE.101.062702)

I. INTRODUCTION

The current trend toward further miniaturization in the drug delivery devices, manipulation of biomolecules and biosensing has brought an increasing number of integrated microdevices for chemical and biological applications [1]. Such a manipulation, for instance, of flow, can be achieved either by forces applied macroscopically, e.g., at appropriate inlets or outlets, or can be generated locally within the microfluidic channel or liquid crystal (LC) cell [2–4]. Electro-osmosis, dielectrophoresis, and electrowetting have been explored for controlling microflows [1–4]. Nematic liquid crystal (NLC) cells of appropriate size are microdevices whose molecular orientations can be manipulated by the presence of electric field \mathbf{E} and the temperature gradient ∇T [5,6]. A challenging problem in all such systems is the precise handling of LC or anisotropic liquid microvolume, which in turn requires self-contained micropumps of small package size exhibiting either a very small displacement volume (displacement pumps) or a continuous volume flow (dynamic pumps). One of the liquid crystal pumping principles is based on the coupling between the electric and director fields, together with accounting the effect of the temperature gradient ∇T [5,7]. In this case, the

uniform textures of nematic LCs are produced by orienting a drop of bulk material in between two conveniently treated bounding surfaces, which define usually a fixed orientation for the boundary molecules. When there is no temperature gradient, applying the electric field \mathbf{E} perpendicular to a uniformly (homogeneously) oriented NLC can distort the molecular orientation $\hat{\mathbf{a}}$ with respect to director $\hat{\mathbf{n}}$, at a critical threshold field E_{th} given by [8]

$$E_{\text{th}} = \frac{\pi}{d} \sqrt{\frac{K_1}{\epsilon_0 \epsilon_a}}, \quad (1)$$

where d is the thickness of the microsized LC channel, K_1 is the splay elastic constant, ϵ_0 is the absolute dielectric permittivity of free space, and ϵ_a is the dielectric anisotropy of the NLC. This form for the critical field is based upon assumption that the director remains strongly anchored (in our case, homogeneously) at the two horizontal bounding surfaces and that the physical properties of the LC are uniform over the entire sample for $E < E_{\text{th}}$. When the electric field is switched on with a magnitude E greater than E_{th} , the director $\hat{\mathbf{n}}$, in the “splay” geometry, reorients as a simple monodomain [5], and exciting of the electrically driven nematic flow in microfluidic channel containing a temperature gradient is a question of great fundamental interest, as well as essential piece of knowledge in soft material science [1]. In the nematic microfluidic channel where director anchoring on the bounding surfaces are the same, i.e., both homogenous, and when the gradient

*alexandre.zakharov@yahoo.ca; www.ipme.ru

†pashamaslennikov@mail.ru

‡s-p-a-s-m@mail.ru

of the temperature field ∇T does not exist, the horizontal flow of the nematic material is excited only by the electric field $\mathbf{E} = E(z)\hat{\mathbf{k}}$ directed orthogonally to the homogeneously aligned LC sample. In turn, accounting the temperature gradient ∇T , generated, for instance, by the uniform heating both from below or above, leads to the additional contributions to the torque and linear momentum balance equations.

Based upon the nonlinear extension of the classical Ericksen-Leslie theory, with accounting the entropy balance equation, the effect of coupling among the ∇T , $\nabla \hat{\mathbf{n}}$, and \mathbf{E} on the electrically driven nematic flow in microfluidic LC channel containing the temperature gradient will be investigated.

The outline of this paper is as follow: The system of hydrodynamic equations describing both the director motion and the fluid flow in microfluidic LC channel containing the temperature gradient under the effect of the external electric field is given in Sec. II. Numerical results for the relaxation regimes, caused both the electric field and the vertical temperature gradient, describing orientational relaxation of the director, velocity, and temperature are given in Sec. III. Conclusions are summarized in Sec. IV.

II. FORMULATION OF THE BALANCE OF THE LINEAR MOMENTUM, TORQUE, AND CONDUCTIVITY EQUATIONS FOR MICROSIZED NEMATIC FLUIDS

We are primarily concerned with the description of the physical mechanism responsible for the electrically driven nematic flow in microfluidic homogeneously aligned liquid crystal (HALC) channels containing a temperature gradient ∇T . This gradient was fixed between two boundaries of this channel, for instance, between the planar warmer upper and planar cooler lower bounding surfaces. As a result, one arrives at the picture where there is a balance between the applied ∇T and the electric, viscous, elastic, and anchoring forces, and, in general, the LC fluid settles down to a stationary flow regime in the horizontal direction [7]. Upon assuming an incompressible fluid, the hydrodynamic equations describing the orientational dynamics induced both by electric field $\mathbf{E} = E\hat{\mathbf{k}}$ and ∇T can be derived from the torque, linear momentum, and the entropy balance equations for such LC system. We consider a homogeneously aligned nematic system such as cyanobiphenyls, which is delimited by two horizontal bounding surfaces at distance d on a scale in the order of tens micrometers (see Fig. 1).

According to this geometry the director is maintained within the xz plane (or in the yz plane) defined by the electric field and the unit vector $\hat{\mathbf{i}}$ directed parallel to the horizontal surfaces, $\hat{\mathbf{k}}$ is a unit vector directed normal to the horizontal surfaces, and $\hat{\mathbf{j}} = \hat{\mathbf{k}} \times \hat{\mathbf{i}}$. Because we deal with the HALC channel under influence both the electric field $\mathbf{E} = E(z)\hat{\mathbf{k}}$ and the temperature gradient ∇T directed perpendicular to the HALC channel, and taking into account that the length of the channel L much bigger than the thickness d , we can suppose that the component of the director $\hat{\mathbf{n}} = n_x\hat{\mathbf{i}} + n_z\hat{\mathbf{k}} = \sin\theta(z, t)\hat{\mathbf{i}} + \cos\theta(z, t)\hat{\mathbf{k}}$ as well as the rest of the physical quantities also depend only on the z coordinate and time t . Here θ denotes the angle between the director and the unit vector $\hat{\mathbf{k}}$.

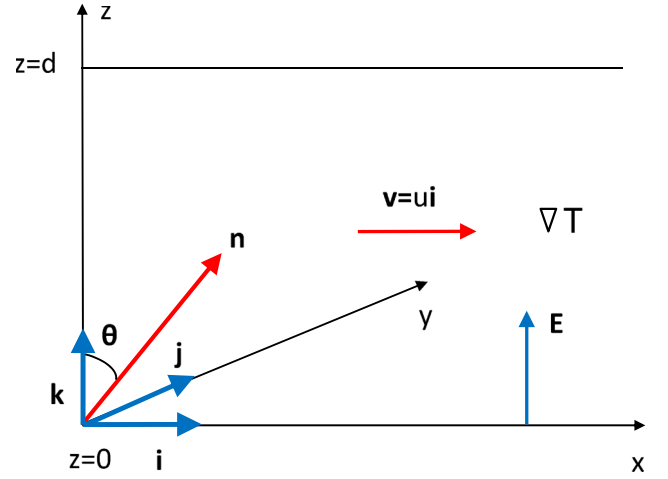


FIG. 1. The coordinate system used for theoretical analysis. The x axis is taken as being parallel to the director directions on the lower and upper surfaces, $\theta(z, t)$ is the angle between the director $\hat{\mathbf{n}}$ and the unit vector $\hat{\mathbf{k}}$, respectively. Both the electric field \mathbf{E} and the unit vector $\hat{\mathbf{k}}$ are directed normal to the horizontal surfaces of the LC channel.

Our main aim is to investigate the influence of the external electric field \mathbf{E} and the heat flux \mathbf{q} , generated by uniform heating both from below or above, on the process of the director reorientation $\hat{\mathbf{n}}$ and electrically driven nematic flow \mathbf{v} in the microfluidic HALC channel containing the temperature gradient. To elucidate the role of both the temperature gradient ∇T and the electric field \mathbf{E} on the reorientation process in the microsized HALC channel, we consider a number of regimes, first, when the LC sample is subjected to uniform heating from below and the director $\hat{\mathbf{n}}$ is strongly anchored to both solid surfaces, planarly to the lower cooler (T_1) and the upper hotter (T_2) bounding surfaces, where

$$\theta(z)_{z=0} = \frac{\pi}{2}, \theta(z)_{z=d} = \frac{\pi}{2},$$

$$T(z)_{z=0} = T_1, T(z)_{z=d} = T_2 (T_2 > T_1). \quad (2)$$

If the director is disturbed by both the electric field \mathbf{E} and the heat flux $\mathbf{q} = -T \frac{\delta \mathcal{R}}{\delta \nabla T}$, generated by the uniform heating both from below or above, then the relaxation of $\hat{\mathbf{n}}(z, t)$ to its equilibrium orientation $\hat{\mathbf{n}}_{\text{eq}}(z)$ in the HALC channel is governed by electric $\mathbf{T}_{\text{el}} = \frac{\delta \psi_{\text{el}}}{\delta \hat{\mathbf{n}}} \times \hat{\mathbf{n}}$, elastic $\mathbf{T}_{\text{elast}} = \frac{\delta \mathcal{W}_{\text{E}}}{\delta \hat{\mathbf{n}}} \times \hat{\mathbf{n}}$, viscous $\mathbf{T}_{\text{vis}} = \frac{\delta \mathcal{R}^{\text{vis}}}{\delta \hat{\mathbf{n}}} \times \hat{\mathbf{n}}$, and thermomechanical $\mathbf{T}_{\text{tm}} = \frac{\delta \mathcal{R}^{\text{tm}}}{\delta \hat{\mathbf{n}}} \times \hat{\mathbf{n}}$ torques exerted per unit LC's volume. Here $\mathcal{R} = \mathcal{R}^{\text{vis}} + \mathcal{R}^{\text{tm}} + \mathcal{R}^{\text{th}}$ is the full Rayleigh dissipation function, \mathcal{R}^{vis} , \mathcal{R}^{tm} , and \mathcal{R}^{th} are the viscous, thermomechanical and thermal contributions to \mathcal{R} , and will be defined below, whereas $\mathcal{W}_{\text{E}} = \frac{1}{2}[K_1(\nabla \cdot \hat{\mathbf{n}})^2 + K_3(\hat{\mathbf{n}} \times \nabla \times \hat{\mathbf{n}})^2]$ denotes the elastic energy densities, K_1 and K_3 are splay and bend elastic coefficients, $\psi_{\text{el}} = -\frac{1}{2}\epsilon_0\epsilon_a(\hat{\mathbf{n}} \cdot \mathbf{E})^2$ is the electric energy density, and $\hat{\mathbf{n}}_t = \frac{d\hat{\mathbf{n}}}{dt}$ is the material derivative of the director $\hat{\mathbf{n}}$, respectively.

The application of the voltage across the nematic film results in a variation of $E(z)$ through the channel which is obtained from [5]

$$\frac{\partial}{\partial z} \left[\left(\frac{\epsilon_{\perp}}{\epsilon_a} + \sin^2 \theta(\tau, z) \right) \bar{E}(z) \right] = 0, \quad 1 = \int_0^d \bar{E}(z) dz, \quad (3)$$

where $\bar{E}(z) = \frac{E(z)}{E}$, $E = \frac{U}{d}$, and U is the voltage applied across the channel, $\epsilon_a = \epsilon_{\parallel} - \epsilon_{\perp}$, ϵ_{\parallel} , and ϵ_{\perp} are the dielectric constants parallel and perpendicular to the director. Note that the overbars in the electric field \bar{E} will be eliminated in the following equations.

The hydrodynamic equations describing the reorientation of the LC phase in our case, when there exists the heat flux \mathbf{q} across the HALC microfluidic channel, can be derived from the torque balance equation [9,10] $\mathbf{T}_{\text{el}} + \mathbf{T}_{\text{elast}} + \mathbf{T}_{\text{vis}} + \mathbf{T}_{\text{tm}} = 0$, which has the form

$$\left[\frac{\delta \psi_{\text{el}}}{\delta \hat{\mathbf{n}}} + \frac{\delta \mathcal{W}_F}{\delta \hat{\mathbf{n}}} + \frac{\delta \mathcal{R}^{\text{vis}}}{\delta \hat{\mathbf{n}}_t} + \frac{\delta \mathcal{R}^{\text{tm}}}{\delta \hat{\mathbf{n}}_t} \right] \times \hat{\mathbf{n}} = 0. \quad (4)$$

The linear momentum equation for the velocity field \mathbf{v} can be written as [9,10]

$$\rho \frac{d\mathbf{v}}{dt} = \nabla \cdot \sigma, \quad (5)$$

where $\sigma = \sigma^{\text{elast}} + \sigma^{\text{vis}} + \sigma^{\text{tm}} - \mathcal{P}\mathcal{I}$ is the full stress tensor (ST), and $\sigma^{\text{elast}} = -\frac{\partial \mathcal{W}_F}{\partial \nabla \hat{\mathbf{n}}} \cdot (\nabla \hat{\mathbf{n}})^T$, $\sigma^{\text{vis}} = \frac{\delta \mathcal{R}^{\text{vis}}}{\delta \nabla \mathbf{v}}$, and $\sigma^{\text{tm}} = \frac{\delta \mathcal{R}^{\text{tm}}}{\delta \nabla \mathbf{v}}$ are the ST components corresponding to the elastic, viscous, and thermomechanical forces, respectively. Here \mathcal{P} is the hydrostatic pressure in the HALC system and \mathcal{I} is the unit tensor, respectively.

When the gradient of temperature ∇T is set up across the HALC channel, we expect that the temperature field $T(z, t)$ satisfies the heat conduction equation [11]

$$\rho C_p \frac{dT}{dt} = -\nabla \cdot \mathbf{q}, \quad (6)$$

where $\mathbf{q} = -T \frac{\delta \mathcal{R}}{\delta \nabla T}$ is the heat flux in the nematic phase, and C_p is the heat capacity of the LC system and ρ is the mass density of the nematic system.

Taking into account the microsize of the HALC channel, one can assume the mass density ρ to be constant over the LC volume, and thus we can deal with an incompressible fluid. The incompressibility condition $\nabla \cdot \mathbf{v} = 0$ assumes that only one nonzero component of the vector \mathbf{v} exists, viz. $\mathbf{v}(z, t) = u(z, t)\hat{\mathbf{i}}$.

To be able to observe the evolution of the director field $\hat{\mathbf{n}}$ [or the polar angle $\theta(z, t)$] to its equilibrium orientation $\hat{\mathbf{n}}_{\text{eq}}(z)$, and exciting the velocity field $\mathbf{v}(z, t)$ caused both by the temperature gradient and the external electric field, we consider the dimensionless analog of the torque and linear momentum balance equations, as well as the entropy balance equation.

The dimensionless torque balance equation describing the reorientation of the LC phase can be written as [5,7]

$$\theta_{\tau} = \mathcal{A}(\theta)u_z + \Delta \left[(\mathcal{G}(\theta)\theta_z)_z - \frac{1}{2}\mathcal{G}_{,\theta}(\theta)\theta_z^2 \right] - \Delta \delta_1 \chi_z \theta_z \left(\frac{1}{2} + \sin^2 \theta \right) - \frac{E^2(z)}{2} \sin 2\theta, \quad (7)$$

here $\mathcal{A}(\theta) = \frac{1}{2}(1 - \gamma_{21} \cos 2\theta)$, $\mathcal{G}(\theta) = \sin^2 \theta + K_{31} \cos^2 \theta$, $\mathcal{G}_{,\theta}(\theta)$ is the derivative of $\mathcal{G}(\theta)$ with respect to θ , $\chi(z, \tau) = T(z, \tau)/T_{NI}$ is the dimensionless temperature, T_{NI} is the nematic-isotropic transition temperature, $\theta_{,z} = \partial \theta(z, \tau)/\partial z$, $\chi_{,z} = \partial \chi(z, \tau)/\partial z$, $\Delta = \left(\frac{E_{th}}{\pi E}\right)^2$, $\gamma_{21} = \gamma_2/\gamma_1$, γ_1 , and γ_2 are

the rotational viscosity coefficients (RVCs), $K_{31} = K_3/K_1$, K_1 , and K_3 are the splay and bend elastic constants of the LC phase, $\tau = (\epsilon_0 \epsilon_a E^2 / \gamma_1) t$ is the dimensionless time, $\bar{z} = z/d$ is the dimensionless distance away from the lower solid surface, $\bar{u} = \left(\frac{\gamma_1}{d \epsilon_0 \epsilon_a E^2}\right) u$ is the dimensionless velocity, $\delta_1 = \xi T_{NI}/K_1$ is the parameter of the system, and $\xi \sim 10^{-12} \text{J/mK}$ is the thermomechanical constant [7]. Notice that the overbars in the space variable z and velocity u have been eliminated. In the case of incompressible fluid the dimensionless Navier-Stokes equation reduces to [5,7]

$$\frac{1}{\Delta} \delta_2 u_{\tau}(z, \tau) = [\bar{h}(\theta)u_z - \bar{\mathcal{A}}(\theta)\theta_{\tau}]_z - \delta_1 \Delta \left[\chi_z \theta_z \sin^2 \theta \left(1 + \frac{1}{2} \sin^2 \theta \right) \right]_z. \quad (8)$$

Here $\mathcal{R}(z, \tau) = \frac{\gamma_1 d^4}{K_1^2} \mathcal{R}(z, t)$ is the full dimensionless Rayleigh dissipation function, where $\mathcal{R}(z, t) = \mathcal{R}^{\text{vis}} + \mathcal{R}^{\text{tm}} + \mathcal{R}^{\text{th}}$, $\mathcal{R}^{\text{vis}} = \frac{1}{2} h(\theta) u_z^2 - \bar{\mathcal{A}}(\theta) \theta_t u_z + \frac{1}{2} \gamma_1 \theta_t^2$ is the viscous, $\mathcal{R}^{\text{tm}} = \xi \theta_t \theta_z T_z \left(\frac{1}{2} + \sin^2 \theta \right) - \xi T_z u_z \theta_z \sin^2 \theta \left(1 + \frac{1}{2} \sin^2 \theta \right)$ is the thermomechanical, and $\mathcal{R}^{\text{th}} = \frac{1}{2T} (\lambda_{\parallel} \cos^2 \theta + \lambda_{\perp} \sin^2 \theta) T_z^2$ is the thermal contributions, respectively. Here $h(\theta) = \alpha_1 \sin^2 \theta \cos^2 \theta - \bar{\mathcal{A}}(\theta) + \frac{1}{2} \alpha_4 + g(\theta)$, $\bar{\mathcal{A}}(\theta) = \gamma_1 \mathcal{A}(\theta)$, $g(\theta) = \frac{1}{2} (\alpha_6 \sin^2 \theta + \alpha_5 \cos^2 \theta)$, $u_z = \partial u(z, t)/\partial z$, $\theta_z = \partial \theta(z, t)/\partial z$, $T_z = \partial T(z, t)/\partial z$, and $\delta_2 = \rho K_1 / \gamma_1^2$ is a parameter of the system. Here α_i ($i = 1, \dots, 6$) are six Leslie coefficients, and λ_{\parallel} and λ_{\perp} are the heat conductivity coefficients parallel and perpendicular to the director $\hat{\mathbf{n}}$, respectively. The stress tensor component σ_{zx} is given by [7] $\sigma_{zx}(\tau) = \frac{\delta \mathcal{R}(\tau)}{\delta u_z} = \bar{h}(\theta) u_z - \mathcal{A}(\theta) \theta_{\tau} - \delta_1 \Delta^2 \chi_z \theta_z \sin^2 \theta \left(1 + \frac{1}{2} \sin^2 \theta \right)$, where $\bar{h}(\theta) = h(\theta)/\gamma_1$. When the temperature gradient ∇T is set up across the HALC channel, we expect that the temperature field $\chi(z, \tau)$ satisfies the dimensionless heat conduction equation [7]

$$\chi_{\tau}(z, \tau) = \delta_3 \Delta [\chi_z (\lambda \cos^2 \theta + \sin^2 \theta)]_z + \delta_4 \left\{ \chi \theta_z \left[\theta_{\tau} \left(\frac{1}{2} + \sin^2 \theta \right) - u_z \sin^2 \theta \left(1 + \frac{1}{2} \sin^2 \theta \right) \right] \right\}_z, \quad (9)$$

where $\lambda = \lambda_{\parallel}/\lambda_{\perp}$, and $\delta_3 = \lambda_{\perp} \gamma_1 / \rho C_p K_1$ and $\delta_4 = \xi / (d^2 \rho C_p)$ are two extra parameters of the system. Note that the overbars in the space variable z in Eqs. (7), (8), and (9) have also been eliminated.

To elucidate the role of both the temperature gradient $\nabla \chi$ and the electric field \mathbf{E} on the reorientation process in the microsized HALC channel, we consider a number of regimes, first, when the director $\hat{\mathbf{n}}$ is strongly anchored to both solid surfaces, planarly to the lower cooler (χ_1) and the upper hotter (χ_2) bounding surfaces, where

$$\theta(z)_{z=0} = \frac{\pi}{2}, \quad \theta(z)_{z=1} = \frac{\pi}{2}, \quad \chi(z)_{z=0} = \chi_1, \quad \chi(z)_{z=1} = \chi_2 (\chi_2 > \chi_1) \text{ (Case I)}, \quad (10)$$

second, when the director $\hat{\mathbf{n}}$ is strongly anchored to both solid surfaces, planarly to the lower hotter (χ_1) and to the upper

cooler (χ_2) bounding surfaces, where

$$\theta(z)_{z=0} = \frac{\pi}{2}, \quad \theta(z)_{z=1} = \frac{\pi}{2},$$

$$\chi(z)_{z=0} = \chi_1, \quad \chi(z)_{z=1} = \chi_2 \quad (\chi_1 > \chi_2) \text{ (Case II)}, \quad (11)$$

third, when the director $\hat{\mathbf{n}}$ is weakly anchored to the upper hotter (χ_2) and strongly (planarly) to the lower cooler (χ_1) bounding surfaces, where

$$\theta(z)_{z=0} = \frac{\pi}{2}, \quad (\partial\theta(z)/\partial z)_{z=1} = \frac{Ad}{2K_1} \sin 2\Delta\theta,$$

$$\chi(z)_{z=0} = \chi_1, \quad \chi(z)_{z=1} = \chi_2 \quad (\chi_2 > \chi_1) \text{ (Case III)}, \quad (12)$$

respectively, and its initial orientation is perturbed parallel to the interface, with

$$\theta(z, \tau = 0) = \frac{\pi}{2}, \quad (13)$$

and then allowed to relax to its equilibrium distribution $\theta_{\text{eq}}(z)$ across the micro-sized HALC channel.

In our case, when the director $\hat{\mathbf{n}}$ is weakly anchored to the upper bounding surface, the anchoring energy W can be written in the form [12] $W = \frac{1}{2}A \sin^2 \Delta\theta$, where A is the anchoring strength, $\Delta\theta = \theta_s - \theta_0$, θ_s and θ_0 are the polar angles corresponding to the director orientation on the upper bounding surface $\hat{\mathbf{n}}_s$ and easy axis $\hat{\mathbf{e}}$, respectively.

The velocity on these surfaces has to satisfy the no-slip boundary condition,

$$u(z)_{z=0} = 0, \quad u(z)_{z=1} = 0. \quad (14)$$

Now the reorientation of the director in the micro-sized HALC channel confined between two solid surfaces, when the relaxation regime is governed by the viscous, electric, elastic, and thermomechanical forces, and with accounting the flow, can be obtained by solving the system of the nonlinear partial differential Eqs. (3), (7), (8), and (9), with the appropriate boundary conditions both for the polar angle $\theta(z, \tau)$ [Eqs. (10)–(12)] and the velocity $u(z, \tau)$ [Eq. (14)], as well as with the initial condition [Eq. (13)].

III. NUMERICAL RESULTS FOR THE RELAXATION REGIMES IN HALC CHANNEL

Here we focus on the problem of how much the coupling between the temperature $\nabla\chi$ and the director $\nabla\hat{\mathbf{n}}$ gradients, as well as the external electric field \mathbf{E} , influences both the direction and magnitude of the hydrodynamic flow \mathbf{v} , excited in the HALC microfluidic channel. In our case the $\nabla\chi$ is produced by the heat flux \mathbf{q} , directed across the HALC channel, whereas the $\nabla\hat{\mathbf{n}}$, in the initially homogeneously aligned microfluidic channel, is set up due to the electric field, which penetrates the bulk of the LC phase.

For the case of 4-cyano-4'-pentylbiphenyl (5CB), at temperature corresponding to nematic phase, the first four parameters of our system of the nonlinear partial differential Eqs. (2), (7), (8), and (9) are $\delta_1 = \xi \frac{T_M}{K_1} = 30.7$, $\delta_2 = \rho K_1 / \gamma_1^2 = 2 \times 10^{-6}$, $\delta_3 = \lambda_{\perp} \gamma_1 / \rho C_p K_1 = 9.23 \times 10^2$, and $\delta_4 = \xi / (d^2 \rho C_p) = 4 \times 10^{-8}$, respectively. For calculations, the value of the density ρ was chosen to be equal to 10^3 kg/m^3 , whereas both the Frank elastic coefficient K_1 and the RVC γ_1 were chosen as $\sim 10 \text{ pN}$ [13] and $\sim 0.071 \text{ Pa s}$ [14],

respectively. The value of the heat conductivity coefficient λ_{\perp} is equal to $\sim 0.24 \text{ W/m K}$ [15], whereas the measured value of the specific heat C_p is equal to $\sim 10^3 \text{ J/kgK}$ [16], respectively.

Accounting the electric field $\mathbf{E} = E\hat{\mathbf{k}}$ directed across the homogeneously aligned nematic channel leads to reorientation of the director field $\hat{\mathbf{n}}$, being initially parallel to the bounding surfaces, to be parallel to \mathbf{E} . Thus, in initially homogeneously aligned LC volume, the hybrid-aligned micro-sized domain may arise, with nonzero gradient of the director field $\nabla\hat{\mathbf{n}}$,

$$\text{Case } E > E_{\text{th}}.$$

In the case when the electric field is equal to $E/E_{\text{th}} = 2.0$ and there is no temperature gradient $\nabla\chi = 0.0$, the evolution of the director field $\hat{\mathbf{n}}$ to its equilibrium orientation $\hat{\mathbf{n}}_{\text{eq}}$ in the micro-sized HALC channel, which is described by the polar angle $\theta(z, \tau_k)$, at different times $\tau_k = \Delta\tau(k-1)$ ($k = 1, \dots, 11$), is shown in Fig. 2(a). Here $\Delta\tau = 0.05$ and $\tau_{11}(E/E_{\text{th}} = 2.0) = 0.5$ ($\sim 2.25 \text{ ms}$). In the calculations, by means of the numerical relaxation method [17], the relaxation criterion $\epsilon = |[\theta_{(m+1)}(z, \tau) - \theta_{(m)}(z, \tau)] / \theta_{(m)}(z, \tau)|$ was chosen to be equal to 10^{-4} , and the numerical procedure was then carried out until a prescribed accuracy was achieved. Here m is the iteration number. In turn, when the electric field is equal to $E/E_{\text{th}} = 2.0$ and the temperature gradient $\nabla\chi \neq 0$ ($\Delta\chi = 0.0162$) is directed from the lower cooler $\chi_1 = 0.97$ ($T_1 = 300 \text{ K}$) to the upper hotter $\chi_2 = 0.9862$ ($T_2 = 307 \text{ K}$) restricted surfaces (case I), the evolution of the director field $\hat{\mathbf{n}}$ to its equilibrium orientation $\hat{\mathbf{n}}_{\text{eq}}$ in the micro-sized HALC channel, which is described by the polar angle $\theta(z, \tau_k)$, at different times $\tau_k = \Delta\tau(k-1)$ ($k = 1, \dots, 11$), is shown in Fig. 2(b). The curves shown on the left-hand side in Fig. 2(a) has been obtained by solving the system of the nonlinear partial differential Eqs. (3), (7), and (8), with $\chi(z, \tau) = 0$, supplemented with appropriate dimensionless boundary Eqs. (10) and (14) and initial Eq. (13) conditions. The curves shown on the right-hand side in Fig. 2(b) (case I) correspond to the polar angle $\theta(z, \tau)$ dependencies calculated taking into account the effect of the electric field $E/E_{\text{th}} = 2.0$, and the temperature gradient $\nabla\chi \neq 0$ is directed from the lower cooler $\chi_1 = 0.97$ ($T_1 = 300 \text{ K}$) to the upper hotter $\chi_2 = 0.9862$ ($T_2 = 307 \text{ K}$) restricted surfaces, has been obtained by solving the system of the nonlinear partial differential Eqs. (3), (7), (8), and (9), with the appropriate dimensionless boundary Eq. (11) and initial Eq. (13) conditions. It should be noted that accounting the heat flux \mathbf{q} leads to asymmetry in the distributions of the polar angle $\theta(z, \tau)$, shifted to the hotter side. Second, based on our calculations, one comes to conclusion that under the influence both the electric field and the heat flux \mathbf{q} , the director's field is more strongly turned toward the unit vector $\hat{\mathbf{k}}$. The influence of the direction of the heat flux \mathbf{q} on the reorientation of the director field is shown in Fig. 3. The curves shown on the right-hand side in Fig. 3(a) correspond to the polar angle $\theta(z, \tau)$ dependencies calculated taking into account both the effect of the electric field $E/E_{\text{th}} = 2.0$ and the heat flux $\mathbf{q} = q\hat{\mathbf{k}}$, when the temperature gradient $\nabla\chi$ is directed from the lower cooler $\chi_1 = 0.97$ ($T_1 = 300 \text{ K}$) to the upper hotter $\chi_2 = 0.9862$ ($T_2 = 307 \text{ K}$) restricted surfaces (case I), and has been obtained by solving the system of the

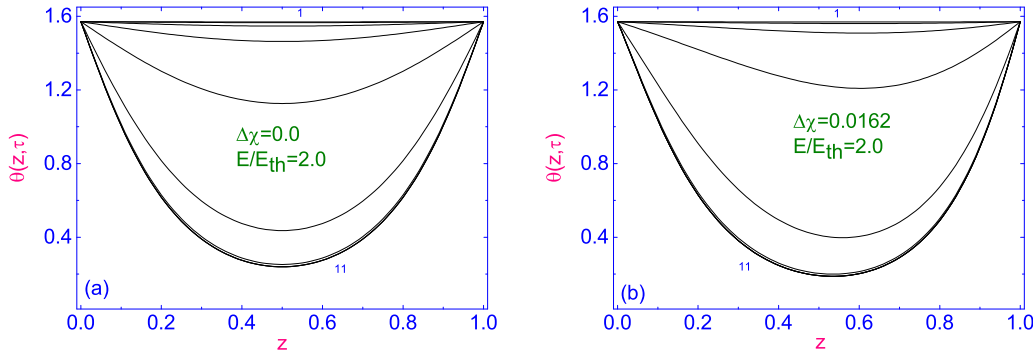


FIG. 2. Plot of the evolution of the polar angle $\theta(z, \tau_k)$ to its equilibrium distribution across the HALC microfluidic channel, under the effect of the electric field $E/E_{th} = 2.0$, at different times $\tau_k = \Delta\tau(k - 1)$ ($k = 1, \dots, 11$), respectively. The curves shown on the left-hand side (a) correspond to the case when $\Delta\chi = 0.0$, whereas the curves shown on the right-hand side (b) correspond to the case when $\Delta\chi = 0.0162$, respectively.

nonlinear partial differential Eqs. (3), (7), (8), and (9), with the appropriate dimensionless boundary Eqs. (10) and (14) and initial Eq. (13) conditions. In turn, the curves shown on the right-hand side in Fig. 3(b) (case II) correspond to the polar angle $\theta(z, \tau)$ dependencies calculated taking into account both the effect of the electric field $E/E_{th} = 2.0$ and the heat flux $\mathbf{q} = -q\hat{\mathbf{k}}$, when the temperature gradient $\nabla\chi$ is directed from the upper cooler $\chi_2 = 0.97$ ($T_2 = 300$ K) to the lower hotter $\chi_1 = 0.9862$ ($T_1 = 307$ K) restricted surfaces, and has been obtained by solving the system of the nonlinear partial differential Eqs. (3), (7), (8), and (9), with the appropriate dimensionless boundary Eqs. (11) and (14) and initial Eq. (13) conditions. First of all, it should be noted that in both cases I and II, accounting the heat flux \mathbf{q} leads to asymmetry in the distributions of the polar angle $\theta(z, \tau)$, shifted to the hotter side. Second, based on our calculations, one comes to the conclusion that the influence of the heat flux \mathbf{q} on the orientation of the director field over the HALC microfluidic channel is negligible in comparison with the electric field $E/E_{th} = 2.0$. Below it will be shown that the main role of the heat flux \mathbf{q} is that it determines the direction of the hydrodynamic flow \mathbf{v} in the HALC microfluidic channel [see Figs. 4(a) and 4(b)]. The evolution of the dimensionless velocity field $u(z, \tau) = (\frac{\gamma_1}{d\epsilon_0\epsilon_s E^2})v_x(z, \tau)$ to its equilibrium distribution $u(z, \tau_{10})$ across the microsized HALC channel,

both in cases I and II, at different times τ_k ($k = 1, \dots, 11$), under the effect of the electric field $E/E_{th} = 2.0$, are shown in Figs. 4(a) and 4(b). The curves shown on the left-hand side in Fig. 4(a) (case I) correspond to the evolution of the dimensionless velocity field $u(z, \tau_k)$ to its equilibrium distribution across the HALC microfluidic channel, both under the effect of the electric field $E/E_{th} = 2.0$ and the heat flux $\mathbf{q} = q\hat{\mathbf{k}}$, directed from the lower cooler $\chi_1 = 0.97$ ($T_1 = 300$ K) to the upper hotter $\chi_2 = 0.9862$ ($T_1 = 307$ K) restricted surfaces, whereas the curves shown on the right-hand side in Fig. 4(b) (case II) correspond to the case when the heat flux $\mathbf{q} = -q\hat{\mathbf{k}}$ is directed from the upper cooler $\chi_2 = 0.97$ ($T_2 = 300$ K) to the lower hotter $\chi_1 = 0.9862$ ($T_1 = 307$ K) restricted surfaces. It is shown, based on our calculations, that changing the direction of the heat flux \mathbf{q} , from the up direction ($\mathbf{q} = q\hat{\mathbf{k}}$) to the down direction ($\mathbf{q} = -q\hat{\mathbf{k}}$), leads to a change in the direction of the hydrodynamic flow $u(z, \tau)$. In case I, when the heat flux $\mathbf{q} = q\hat{\mathbf{k}}$ is directed from the lower cooler to the upper hotter restricted surfaces, the hydrodynamic flow is directed in the negative sense as $\mathbf{v}(z, t) = -u(z, t)\hat{\mathbf{i}}$, whereas in case II, when the heat flux $\mathbf{q} = -q\hat{\mathbf{k}}$ is directed from the upper cooler to the lower hotter restricted surfaces, the hydrodynamic flow is directed in the positive sense as $\mathbf{v}(z, t) = u(z, t)\hat{\mathbf{i}}$. In the first case (case I) when the direction of the heat flux $\mathbf{q} = q\hat{\mathbf{k}}$ coincides with direction of the electric field ($\mathbf{E} = E\hat{\mathbf{k}}$), the ab-

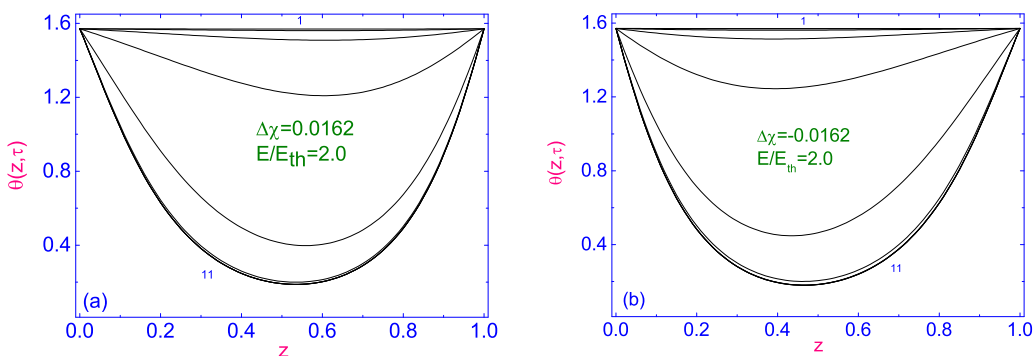


FIG. 3. Plot of the evolution of the polar angle $\theta(z, \tau_k)$ to its equilibrium distribution across the HALC microfluidic channel, both under the effect of the electric field $E/E_{th} = 2.0$ and the heat flux \mathbf{q} , at different times $\tau_k = \Delta\tau(k - 1)$ ($k = 1, \dots, 11$), respectively. The curves shown on the left-hand side (a) correspond to case I, when $\mathbf{q} = q\hat{\mathbf{k}}$, whereas the curves shown on the right-hand side (b) correspond to case II, when $\mathbf{q} = -q\hat{\mathbf{k}}$, respectively.

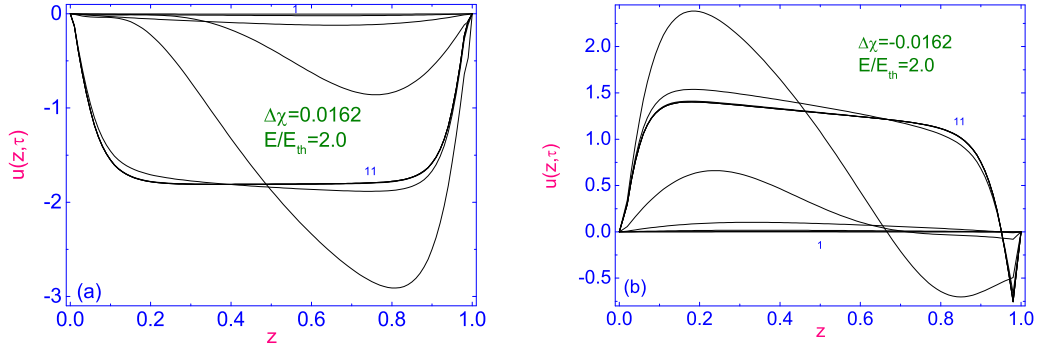


FIG. 4. Plot of the evolution of the dimensionless velocity field $u(z, \tau_k)$ to its equilibrium distribution across the HALC microfluidic channel, under the effect of the electric field $E/E_{th} = 2.0$, at different times $\tau_k = \Delta\tau(k - 1)$ ($k = 1, \dots, 11$), respectively. The curves shown on the left-hand side (a) correspond to case I, when $\mathbf{q} = q\hat{\mathbf{k}}$, whereas the curves shown on the right-hand side (b) correspond to case II, when $\mathbf{q} = -q\hat{\mathbf{k}}$, respectively.

solute value of the hydrodynamic flow $|u(z, \tau)|$ is greater than in case II, when these contributions partially compensate for each other. In case I, the highest velocity value $|u_{max}(E/E_{th} = 2.0)| \sim 2.92$ ($\sim 3.24 \times 10^{-3}$ m/s) is reached near the hotter upper ($z = 0.8$) restricted surface, whereas in case II, the highest velocity value $|u_{max}(E/E_{th} = 2.0)| \sim 2.32$ ($\sim 2.58 \times 10^{-3}$ m/s) is reached near the hotter lower ($z = 0.185$) restricted surface. The evolution of the dimensionless temperature field $\chi(z, \tau) = T(z, \tau)/T_{Nl}$ to its equilibrium distribution $\chi(z, \tau_{11})$ across the microsized HALC channel, both in cases I and II, at different times τ_k ($k = 1, \dots, 11$), are shown in Figs. 5(a) and 5(b). In both cases I and II, we have an almost linear distribution of the temperature field $\chi(z, \tau)$ across the microsized HALC channel.

It should be noted that in the case when the electric field is equal to $E/E_{th} = 2.0$, the value of voltage across the $5\text{-}\mu\text{m}$ -thick LC channel, is equal to 2.12 V.

As the magnitude of the electric field increases, up to $E/E_{th} = 8.0$ and 10.0 , respectively, the picture of the evolution of the director's field changes. In initially homogeneously aligned LC volume, the bigger hybrid-aligned microsized domain may arise, with nonzero gradient of the director field $\nabla\hat{\mathbf{n}}$. In the case when the temperature gradient $\nabla\chi \neq 0$ [$\Delta\chi = 0.0162$ (~ 7 K)], and the value of the electric field increases to $E/E_{th} = 8.0$ and 10.0 , respectively, the evolution of the director field $\hat{\mathbf{n}}$ to its equilibrium orientation $\hat{\mathbf{n}}_{eq}$ in the microsized HALC channel, which is

described by the polar angle $\theta(z, \tau_k)$, at different times $\tau_k = \Delta\tau(k - 1)$ ($k = 1, \dots, 11$), are shown in Figs. 6(a) and 7(a). Here $\Delta\tau = 0.05$ and $\tau_{11}(E/E_{th} = 8.0) = 0.5$ (~ 0.14 ms), whereas $\tau_{11}(E/E_{th} = 10.0) = 0.5$ (~ 0.09 ms), respectively.

First of all, it should be noted that accounting the stronger electric field $E/E_{th} = 8.0$ and 10.0 , respectively, directed across the homogeneously aligned nematic channel leads to reorientation of the most part of the central domain of the LC volume along the direction of the electric field $\mathbf{E} = E\hat{\mathbf{k}}$. Second, with increasing of the electric field up to values of 8.0 and 10.0 , accounting or not accounting the temperature gradient $\nabla\chi$ practically does not affect the final distribution of the director field $\hat{\mathbf{n}}$ across the microsized HALC channel, although the intermediate profiles of the polar angle $\theta(z, \tau_k)$, with $k = 1, \dots, 5$ retain asymmetry [see Figs. 6(a) and 7(a)].

The curves shown in Figs. 6(c) and 7(c) (case A) correspond to the evolution of the dimensionless velocity field $u(z, \tau_k)$ to its equilibrium distribution across the HALC microfluidic channel, both under the effect of the stronger electric field $E/E_{th} = 8.0$ and 10.0 , respectively, and the heat flux $\mathbf{q} = q\hat{\mathbf{k}}$, directed from the lower cooler $\chi_1 = 0.97$ ($T_1 = 300$ K) to the upper hotter $\chi_2 = 0.9862$ ($T_2 = 307$ K) restricted surfaces, whereas the curves shown in Figs. 6(d) and 7(d) (case AA) correspond to the evolution of the dimensionless velocity field $u(z, \tau_k)$ to its equilibrium distribution across the HALC microfluidic channel, under the effect of only the stronger electric field $E/E_{th} = 8.0$ and 10.0 ,

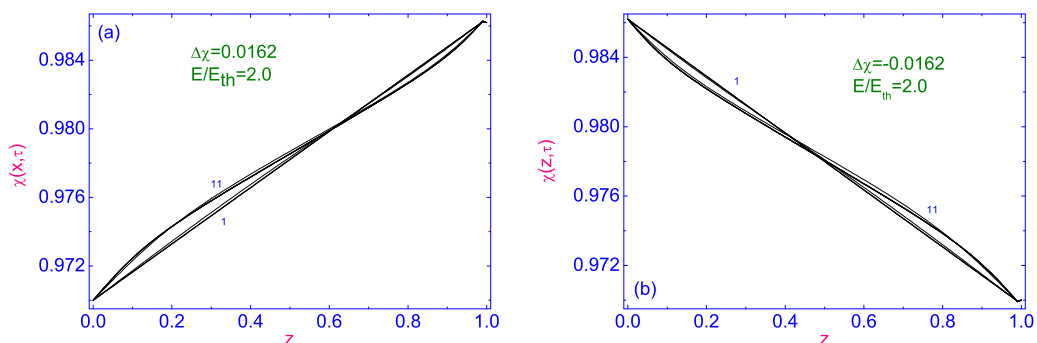


FIG. 5. Same as described in the caption of Fig. 4, but a plot of the evolution of the temperature field $\chi(z, \tau)$ to its equilibrium distribution across the HALC microfluidic channel.

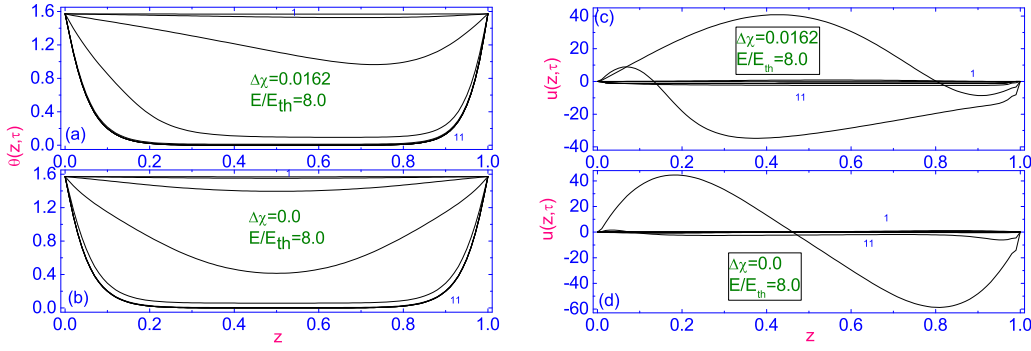


FIG. 6. Plot of the evolution of the polar angle $\theta(z, \tau_k)$ (a) and the dimensionless velocity field $u(z, \tau_k)$ (c) to their equilibrium distributions across the HALC microfluidic channel, both under the effect of the electric field $E/E_{th} = 8.0$ and the heat flux $\mathbf{q} = q\hat{\mathbf{k}}$. (b), (d) Same as in panels (a) and (c), respectively, but there is no temperature gradient $\nabla\chi = 0.0$.

when there is no temperature gradient $\nabla\chi = 0.0$. In case A, the highest velocity value $|u_{\max}(E/E_{th} = 8.0)| \sim 40.0$ (~ 0.71 m/s) and $|u_{\max}(E/E_{th} = 10.0)| \sim 120.0$ (~ 3.34 m/s), respectively, whereas in case AA, the highest velocity value are: $|u_{\max}(E/E_{th} = 8.0)| \sim 55.0$ (~ 0.98 m/s) and $|u_{\max}(E/E_{th} = 10.0)| \sim 27.0$ (~ 0.75 m/s), respectively.

Equilibrium distribution of the velocity profile $u[z, \tau_{11} = u_{eq}(z)]$ across the microsized HALC channel, both under the effect of the electric field E/E_{th} , for the number of values 2.0, 4.0, 8.0, and 10.0, and the heat flux $\mathbf{q} = q\hat{\mathbf{k}}$, directed from the lower cooler $\chi_1 = 0.97$ ($T_1 = 300$ K) to the upper hotter $\chi_2 = 0.9862$ ($T_2 = 307$ K) restricted surfaces, is shown in Fig. 8(a). Our calculations have shown that as the electric field increases greater than $E/E_{th} = 2.0$, the velocity profiles $|u(z, \tau_{11}) = u_{eq}(z)|$ gradually decrease. The dependence of the maximum value of the absolute equilibrium velocity $|u_{\max}(E/E_{th})|$ on the value of electric field E/E_{th} , for the number of regimes is shown in Fig. 8(b). First of all, it should be noted that when calculating the first two curves [curves 1 (case B) and 2 (case BB), Fig. 8(b)], the influence of electric field \mathbf{E} was taken into account using Eq. (1), while when calculating curve 3 (case BBB) [Fig. 8(b)], it was used the relation $E = U/d$, where U is the voltage applied across the LC channel. Second, the first (case B) and third (case BBB) curves were calculated for the case when the director $\hat{\mathbf{n}}$ is strongly anchored to both solid surfaces, planarly to the lower cooler and the upper hotter bounding surfaces, whereas the second curve (case BB) was calculated for the case when the

director $\hat{\mathbf{n}}$ is weakly anchored to the upper hotter and strongly (planarly) to the lower cooler bounding surfaces. For the case of 5CB, at temperature corresponding to nematic phase, the combination $Ad/2K_1$ is approximately equal to 0.1.

Our calculations have shown that the dependence of the maximum value of the absolute equilibrium velocity $|u_{\max}(E/E_{th})|$ on the value of electric field E/E_{th} is characterized by the monotonic increase of $|u_{\max}(E/E_{th})|$ up to maximum value 1.66 at $E/E_{th} \sim 2.0$, whereas further increase of the value of E/E_{th} leads to decrease in $|u_{\max}(E/E_{th})|$. Such behavior of $|u_{\max}(E/E_{th})|$ versus E/E_{th} can be explained by the rapid growth of the coefficient $1/\Delta = (\frac{\pi E}{E_{th}})^2$, in the left-hand side of Eq. (8), with the growth of E/E_{th} . In this case, the contribution of electric forces prevails over the contributions of viscous, elastic, and thermomechanical forces. In this case, any horizontal flow of the LC phase stops in the microsized HALC channel, since under the influence of strong external electric field \mathbf{E} the dipoles of molecules forming the LC phase are oriented along this field. This once again shows that the macroscopic description of the nature of the hydrodynamic flow of an anisotropic liquid subtly senses the microscopic structure of the LC material. In this case, any horizontal flow of the LC phase stops in the microsized HALC channel, since under the influence of strong external electric field \mathbf{E} , the dipoles of molecules forming the LC phase are oriented along this field. This once again shows that the macroscopic description of the nature the hydrodynamic flow of an anisotropic liquid subtly senses the microscopic

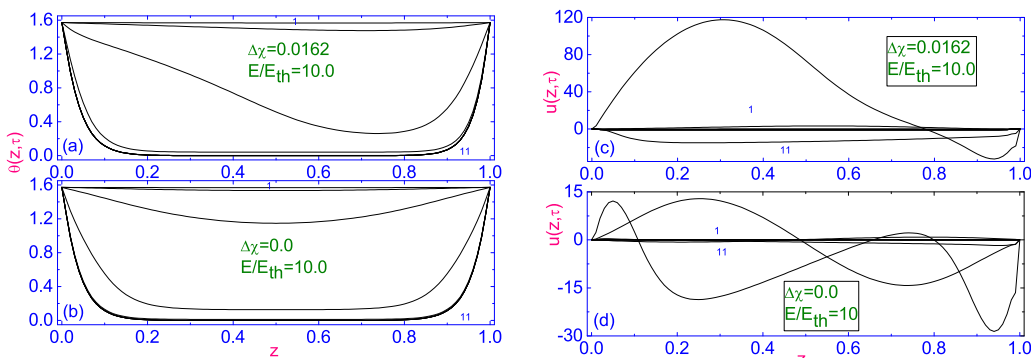


FIG. 7. Same as described in the caption of Fig. 6, but the value of the electric field E/E_{th} is equal to 10.0

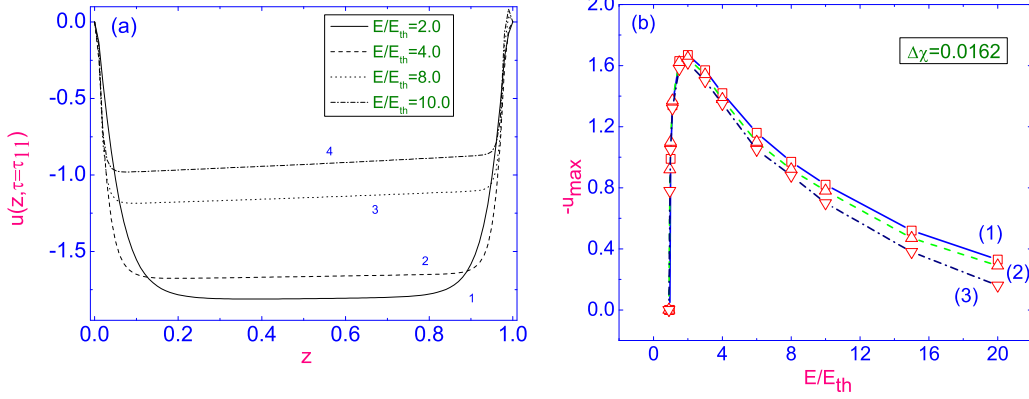


FIG. 8. (a) Plot of the equilibrium dimensionless velocity $u(z, \tau_{11}) = u_{eq}(z)$ vs. the dimensionless space coordinate z , both under the effect of the heat flux $\mathbf{q} = q\hat{\mathbf{k}}$, directed from the lower cooler to the upper hotter restricted surfaces, and the electric field $E/E_{th} = 2.0$ (curve 1), 4.0 (curve 2), 8.0 (curve 3), and 10.0 (curve 4). (b) Dependence of the maximum value of the absolute equilibrium velocity $|u_{max}(E/E_{th})|$ on the value of the electric field E/E_{th} , for the number of regimes, cases B (curve 1), BB (curve 2), and BBB (curve 3).

structure of the LC material,

$$\text{Case } E \gg E_{th}.$$

In the case when the electric field E is much greater than E_{th} , the evolution of the velocity field $u(z, \tau)$ in the microsized HALC channel is described by the reduced dimensionless Navier-Stokes Eq. (8), which can be written as

$$\lim_{E \rightarrow \infty} \frac{1}{\Delta} \delta_2 u, \tau(z, \tau) \rightarrow \infty, \quad (15)$$

where $1/\Delta = (\frac{\pi E}{E_{th}})^2$. In this case when $\lim_{E \rightarrow \infty} \frac{1}{\Delta} \rightarrow \infty$, one has, with accounting the no-slip boundary condition [see Eq. (14)], that $u(z, \tau) = 0$. As a result, in the case when $E \rightarrow \infty$, the dimensionless torque balance Eq. (7) is reduced to equation

$$\theta_\tau(z, \tau) = -\frac{E^2(z)}{2} \sin 2\theta(z, \tau). \quad (16)$$

By substitutions $\bar{\theta} = 2\theta$ and $\beta = E^2\tau$, the last equation takes the form

$$\bar{\theta}_\beta(z, \beta) = -\sin \bar{\theta}. \quad (17)$$

There is exact solution of Eq. (17)

$$\bar{\theta}(z, \beta) = \tan^{-1}[\sinh^{-1}(w\beta - z + z_0)], \quad (18)$$

where z_0 is a constant, and w is the solitary wave velocity along the axis z . Indeed, $\partial_\beta \bar{\theta}(z, \beta) = -\cosh^{-1}(w\beta - z + z_0)$, and taking into account the relation $\tan \bar{\theta}(z, \beta) = \sinh^{-1}(w\beta - z + z_0) = \mathcal{A}$, one has that $\sin \bar{\theta}(z, \beta) = \mathcal{A}/\sqrt{1 + \mathcal{A}^2} = \cosh^{-1}(w\beta - z + z_0)$. Finally, one can rewrite Eq. (17) in the following way: $\partial_\beta \bar{\theta}(z, \beta) = -\cosh^{-1}(w\beta - z + z_0) = -\sin \bar{\theta}(z, \beta)$. Solution Eq. (18) describes the solitary kink $\bar{\theta}(z, \beta)$ which is spreading along the z axis with the velocity

$$w(z, t) = \frac{E^2 \bar{E}(z) d \epsilon_a \epsilon_0}{\gamma_1} = \frac{1}{\Delta} \frac{K_1}{d \gamma_1} \bar{E}(z), \quad (19)$$

where $\bar{E}(z) = E(z)/E$, $E = U/d$, and U is the voltage applied across the LC channel. Physically, this means that in the case $E \gg E_{th}$, directed across the HALC channel, the director field

$\hat{\mathbf{n}}$ has initially been disturbed, for instance, at the bottom of the LC channel, with the condition $\theta(z_0 = 0, \tau = 0) = \frac{\pi}{2}$, and that disturbance must propagate in the form of the solitary wave along the z axis with the velocity w . For instance, when the electric field $E = 100E_{th}$ ($U \sim 106V$) is applied across the HALC channel $5 \mu\text{m}$ thick, the solitary wave velocity w along the z axis is equal to 2.87 m/s.

IV. CONCLUSION

The nonmechanical method for producing flow in a microfluidic homogeneously aligned liquid crystal (HALC) channel containing a temperature gradient ∇T under the effect of the external electric field \mathbf{E} has been proposed. Fluid pumping principle is based on the coupling between the electric and director fields, together with accounting the effect of the temperature gradient ∇T . In the nematic microfluidic channel where director anchoring on the bounding surfaces are the same, i.e., both homogeneous, and when the gradient of the temperature field ∇T does not exist, the horizontal flow of the nematic material is excited only by the electric field $\mathbf{E} = E(z)\hat{\mathbf{k}}$ directed orthogonally to the homogeneously aligned LC sample. In turn, accounting the temperature gradient ∇T leads to the additional contributions both to the torque and linear momentum balance equations. Calculations, based upon the nonlinear extension of the classical Ericksen-Leslie theory, with accounting the entropy balance equation, show that due to the coupling among the ∇T , $\nabla \hat{\mathbf{n}}$, and \mathbf{E} in the HALC microfluidic channel the horizontal flow $\mathbf{v} = v_x \hat{\mathbf{i}} = u \hat{\mathbf{i}}$ may be excited. The direction and magnitude of \mathbf{v} is influenced both by the heat flux \mathbf{q} across the microfluidic channel and the strength of the electric field \mathbf{E} . The results of calculations showed that the dependence of the maximum value of the equilibrium velocity distribution $|u_{max}(E/E_{th})|$ across the LC channel versus electric field E/E_{th} is characterized by maximum value at $E/E_{th} = 2.0$. In the case when the electric field $E \gg E_{th}$, the horizontal flow of the LC material completely stops and a novel mechanism of converting of the electric field in the form of the kinklike wave reorientation of the director field $\hat{\mathbf{n}}$ can be excited in the LC channel.

Physically, this means that in the case $E \gg E_{th}$, directed across the HALC channel, the director field $\hat{\mathbf{n}}$ has initially been disturbed, for instance, at the bottom of the LC channel, and that disturbance must propagate in the form of the kinklike wave across the LC channel.

Notes that the relaxation behavior of the director field $\hat{\mathbf{n}}$ in the form of the kinklike wave $\bar{\theta}(z, \beta)$ which is spreading along the z axis with the velocity w , probably can be observed in polarized white light. Taking into account that the director reorientation takes place in the narrow area of the LC sample (the width of the kinklike wave) under influence of the electric field \mathbf{E} , for instance, $E = 100E_{th}$ or $U \sim 106V$ across the $5 \mu\text{m}$ nematic 5CB channel, the kinklike wave can be visualized in polarized white light as a dark strip running along the normal to both bounding surfaces, with the velocity $w \sim 2.87 \text{ m/s}$.

It should be noted that the role of temperature gradient in formation of the number of nematorheological regimes, using the Ericksen-Leslie (EL) theory, under isothermal condition (without accounting the entropy balance equation) and without the external electric field, has been investigated [18]. It was shown that the EL theory is able to describe a number of rheological regimes, including alignment and tumbling behavior in the shear flow for polar LC compound, such as

4-cyano-4'-octylbiphenyl (8CB) [19]. It was shown that the director field $\hat{\mathbf{n}}$ can be oriented in two ways under the action of the shear flow \mathbf{v} . First, the hydrodynamic torque, exerted per unit LC volume, vanishes when the director aligns at an equilibrium angle $\theta_{eq} = \cos^{-1}(-\gamma_1/\gamma_2)$, with respect to the velocity \mathbf{v} . Second, the director continuously rotates in the shear plane. Taking into account that both coefficients γ_1 and γ_2 are temperature dependent functions, one should expect that some LC materials undergo a transition from an aligning regime to a tumbling instability in the vicinity of a second order nematic-smectic A phase transition temperature [19,20]. But we are dealing with a typical aligning nematic (5CB), and in our case a strong transverse electric field tends to orient the director's field along this field.

This once again shows that the macroscopic description of the nature of the hydrodynamic flow of an anisotropic liquid subtly senses the microscopic structure of the LC material.

ACKNOWLEDGMENT

We acknowledge financial support of the Ministry of Education and Science of the Russian Federation (Grant No. FSFZ-2020-0019). The reported study also was funded by RFBR and DFG, Project No. 20-52-12040.

-
- [1] R. B. Schoch, J. Han, and P. Renaud, *Rev. Mod. Phys.* **80**, 839 (2008).
 - [2] A. Ajdari, *Phys. Rev. E* **61**, R45 (2000).
 - [3] D. Long and A. Ajdari, *Eur. Phys. J. E* **4**, 29 (2001).
 - [4] M. Z. Bazant and Y. Ben, *Lab Chip* **6**, 1455 (2006).
 - [5] A. A. Vakulenko and A. V. Zakharov, *Phys. Rev. E* **88**, 022505 (2013).
 - [6] A. V. Zakharov and P. V. Maslennikov, *Phys. Rev. E* **96**, 052705 (2017).
 - [7] A. V. Zakharov and A. A. Vakulenko, *J. Chem. Phys.* **127**, 084907 (2007).
 - [8] P. G. de Gennes and J. Prost, *The Physics of Liquid Crystals* 2nd. ed. (Oxford University Press, Oxford, 1995).
 - [9] J. L. Ericksen, *Arch. Ration. Mech. Anal.* **4**, 231 (1960).
 - [10] F. M. Leslie, *Arch. Ration. Mech. Anal.* **28**, 265 (1968).
 - [11] L. D. Landau and E. M. Lifshitz, *Fluid Mechanics* (Pergamon Press, Oxford, 1987).
 - [12] A. Rapini and M. Papoular, *J. Phys. Colloq. (France)* **30**, C4-54 (1969).
 - [13] N. V. Madhusudana and R. B. Ratibha, *Mol. Cryst. Liq. Cryst.* **89**, 249 (1982).
 - [14] A. G. Chmielewski, *Mol. Cryst. Liq. Cryst.* **132**, 339 (1986).
 - [15] M. Marinelli, A. K. Ghosh, and F. Mercuri, *Phys. Rev. E* **63**, 061713 (2001).
 - [16] P. Jamee, G. Pitsi, and J. Thoen, *Phys. Rev. E* **66**, 021707 (2002).
 - [17] I. S. Berezin and N. P. Zhidkov, *Computing Methods*, 4th ed. (Pergamon Press, Oxford, 1965).
 - [18] W. H. Han and A. D. Rey, *J. Rheol.* **39**, 301 (1995).
 - [19] R. G. Larson, *The Structure and Rheology of Complex Fluids* (Oxford University Press, Oxford, 1999).
 - [20] A. V. Zakharov and J. Thoen, *Phys. Rev. E* **69**, 051709 (2004).